Short Communication

Development of a finite element analysis program for thin plate plane stress analysis

Michael Dodman[1]

[1]Department of Mechanical Engineering, University College London, Torrington Place, London WC1E 7JE, UK

Corresponding author:
Michael Dodman,
Department of Mechanical Engineering,
University College London,
Torrington Place,
London WC1E 7JE, UK
Email: zcemmrd@ucl.ac.uk

Word count (Introduction through Discussion): 2212

Abstract:
In this paper, a MATLAB implementation of 3-noded and 6-noded triangular elements is constructed to find the displacement and strain in a thin plate in plane stress. This solution is verified in ANSYS Mechanical APDL, showing negligible error. It was found that the 6-noded elements showed significantly higher amounts of nodal deformation and strain than the 3-noded model. Furthermore, using the 6-noded element configuration, an investigation into the effect of strain and displacement with varying Young's Moduli and uniform tension loading angles showed that nodal displacement and element strain are both inversely proportional to Young's Modulus. However, a mesh convergence study showed that three elements are not grid independent, and in fact grid independence was reached at 5181 elements.

Key words: Finite element analysis, plane stress, thin plate, MATLAB, ANSYS Mechanical APDL

Introduction:

Finite element analysis (FEA) is the most used computational tool in science and engineering applications (Ferreira, 2009). Originally, FEA has roots in framed aerospace structures, where it provided solutions as matrix relationships between forces and displacements (Khennane, 2013). FEA has grown to become a general method of numerically solving differential equations for a large range of engineering and mathematical modelling applications.

In the field of structural analysis, FEA is used to simulate structures before production. This allows engineers to determine any design modifications necessary to meet design requirements (Vanam, 2012). The structure can be analysed under varying loads to find out if it can perform in its intended environment. As opposed to real prototyping, FEA allows for relatively much faster, more cost efficient, and safer testing; the adaptive procedures of an FEA software encourage iterative correction. (Akin, 2010). Models are discretized with nodes and elements which allows FEA to cope smoothly with arbitrary shapes, differing boundary conditions and a variety of material properties. FEA is therefore an essential tool in calculating model displacement and strain under load, which is a problem often found in structural engineering.

The utility of FEA has led to most institutions teaching it up to graduate level (W. E. Howard, 2001). Exposure in the form of conducting FEA from first principles is beneficial for students, as well as practicing FEA packages such as ANSYS. However, the cost of commercial packages for those willing to learn, but are without an institution, is certainly a barrier to entry. Programming languages such as MATLAB are also capable of performing FEA and are common in industry (Rao, 2017), but are much more accessible for students of any background. In which case, it is crucial that students take the opportunity to program FEA for themselves.

In this paper, MATLAB is used to solve for the displacement and strain of a thin plate under uniform tension. Firstly, the plate is modelled with three 3-noded triangular elements and then three 6-noded triangular elements. The constructed program is then verified with differing material properties and loading conditions for the 6-noded model. Finally, both the 3

and 6-noded models, as well as a meshed plate, are implemented in ANSYS Mechanical APDL, which is used to validate the MATLAB program.

Materials and Methods:

Details of the model geometry, chosen material properties and boundary conditions are given in this section. The finite element method implemented is also described and the mesh convergence is provided.

Thin Plate Model Description: The model geometry, shown in Figure 1, is a thin plate in plane stress with a 0.04m width and 0.03m height. In the upper right-hand corner, there is a quarter-hole of radius 0.01m, and the plate has a thickness of 0.002m, and so it is treated as a 2D geometry. A uniform tension of magnitude 200 MPa acts on the right-hand side of the geometry at angle θ to the vertical y axis. Furthermore, the bottom left-hand corner is pin supported such that displacement in both degrees of freedom is 0 $(u_x = u_y = 0)$ and the top left-hand corner is roller supported, preventing displacement in the x axis only $(u_x = 0)$. The plate is assumed to be elastic, linear and isotropic with a Young's Modulus of $E = 100$ Gpa and Poisson's Ratio $\nu = 0.3$ in the base case. Additional Young's Moduli and loading directions are tested; $E = \{50, 100, 150, 200, 250\}$ GPa and $\theta = \{0°, 30°, 60°, 90°, 120°\}$, while keeping all other parameters fixed.

Finite Element Method Simulations: Two element configurations are used, namely constant strain triangles (CSTs) and linear strain triangles (LSTs). A CST has three total nodes per triangle while an LST has six due to the addition of three mid-side nodes. These additional mid-side nodes allow for curved element edges (Seshu, 2003). Separate models are created, each with three LSTs or CSTs which incurs the assumption of replacing the quarter-hole with a straight like between node 3 and 4. Figure 2 shows the configurations for both the three-noded and six-noded triangular elements. In ANSYS Mechanical APDL, to replicate the above element regimes, PLANE182 and PLANE183 element types were chosen for CST and LST respectively (Ansys Inc., 2011). The resultant displacement and strain values can then be compared between the MATLAB and ANSYS solutions. A third configuration is constructed in ANSYS Mechanical APDL as part of a grid independence study. The LST thin plate model is meshed with PLANE183 elements with differing global element edge lengths; $L = \{0.02, 0.015, 0.01, 0.005, 0.001, 0.0005\}$ metres. Subsequently, the displacement of nodes 4 and 5 are inspected for convergence at a certain element edge length. Additionally, the Young's Modulus and uniform tension loading direction, θ, are varied for the six-noded model, with all other variables constant, to test the sensitivity of displacement and strain, for E and θ.

Three-Noded Elements: To determine the strain and displacement of the global three-noded model, the functions for each individual element must first be evaluated. In the case of a CST, the characteristic matrices for each element strictly have a linear relationship with x and y. Firstly, the shape functions N_β are given by,

$$N_\beta = \frac{1}{2A}(a_\beta + b_\beta x + c_\beta y), \beta = i, j, k, \quad (1)$$

where β is the node index for a given element, (x, y) are the coordinates of each node, A is the surface area of the element and a, b, c are defined as,

$$\begin{array}{lll} a_i = x_j y_k - x_k y_j & b_i = y_j - y_k & c_i = x_k - x_j \\ a_j = x_k y_i - x_i y_k & b_j = y_k - y_i & c_j = x_i - x_k \\ a_k = x_i y_j - x_j y_i & b_k = y_i - y_j & c_k = x_j - x_i \end{array} \quad (2)$$

Subsequently, A is given by,

$$A = \frac{1}{2}\begin{vmatrix} 1 & x_i & y_i \\ 1 & x_j & y_j \\ 1 & x_k & y_k \end{vmatrix} = \frac{1}{2}\left(x_i y_j + x_j y_k + x_k y_i - x_i y_k - x_j y_i - x_k y_j\right). \quad (3)$$

The system has two degrees of freedom, so the displacement field of each element is calculated as a function of the nodal displacement,

$$u = N_i u_i + N_j u_j + N_k u_k \quad (4)$$

$$v = N_i v_i + N_j v_j + N_k v_k \quad (5)$$

Hence, the non-zero strains for this two-dimensional model are $\varepsilon_x = \frac{\partial u}{\partial x}$, $\varepsilon_y = \frac{\partial u}{\partial x}$ and $\gamma_{xy} = \frac{\partial u}{\partial x} + \frac{\partial v}{\partial y}$. Therefore, the strain-displacement relation matrix $[B]$, for each element is given by,

$$[B] = \frac{1}{2A}\begin{bmatrix} b_i & 0 & b_j & 0 & b_k & 0 \\ 0 & c_i & 0 & c_j & 0 & c_k \\ c_i & b_i & c_j & b_j & c_k & b_k \end{bmatrix}, \quad (6)$$

where $\{U\}$ is the node displacement field.

Finally, the stress-strain relation matrix, $[D]$, for a system in plane stress, is defined as,

$$[D] = \frac{E}{1 - v^2}\begin{bmatrix} 1 & v & 0 \\ v & 1 & 0 \\ 0 & 0 & \frac{1 - v}{2} \end{bmatrix}, \quad (7)$$

leading to the expression for the stiffness matrix for each element,

$$[k]^e = \int_V [B]^T [D][B] dV = [B]^T [D][B] tA, \quad (8)$$

where t is the thickness of the thin plate.

Six-Noded Elements: The finite element formulation of a 6-noded element is non-linear. This means that the strain and displacement matrices have a quadratic relationship with x and y displacements. Hence, the shape functions for each node are given as,

$$
\begin{aligned}
N_1 &= L_1(2L_1 - 1) & N_4 &= 4L_1L_2 \\
N_2 &= L_2(2L_2 - 1) & N_5 &= 4L_2L_3 = 4L_2(1 - L_1 - L_2) \\
N_3 &= L_3(2L_3 - 1) = (1 - L_1 - L_2)(1 - 2L_1 - 2L_2) & N_6 &= 4L_3L_1 = 4L_1(1 - L_1 - L_2)
\end{aligned} \qquad (9)
$$

where L_1, L_2 and L_3 are not independent: $L_1 + L_2 + L_3 = 1$.

Since the above shape functions are given in a natural coordinate system, a Jacobian Matrix is used to transform each element's shape function to the global coordinate system. For a 6-noded isoparametric element, this transformation is given by,

$$
[J] = \begin{bmatrix} \sum_{i=1}^{6} \frac{\partial N_i}{\partial L_1} x_i & \sum_{i=1}^{6} \frac{\partial N_i}{\partial L_1} y_i \\ \sum_{i=1}^{6} \frac{\partial N_i}{\partial L_2} x_i & \sum_{i=1}^{6} \frac{\partial N_i}{\partial L_2} y_i \end{bmatrix}, \qquad (10)
$$

from which the strain-displacement relation matrix $[B]$ for a six-noded element can be expressed as,

$$
[B] = \frac{1}{2A} \begin{bmatrix} \frac{\partial N_1}{\partial x} & 0 & \frac{\partial N_2}{\partial x} & 0 & \frac{\partial N_3}{\partial x} & 0 & \frac{\partial N_4}{\partial x} & 0 & \frac{\partial N_5}{\partial x} & 0 & \frac{\partial N_6}{\partial x} & 0 \\ 0 & \frac{\partial N_1}{\partial y} & 0 & \frac{\partial N_2}{\partial y} & 0 & \frac{\partial N_3}{\partial y} & 0 & \frac{\partial N_4}{\partial y} & 0 & \frac{\partial N_5}{\partial y} & 0 & \frac{\partial N_6}{\partial y} \\ \frac{\partial N_1}{\partial y} & \frac{\partial N_1}{\partial x} & \frac{\partial N_2}{\partial y} & \frac{\partial N_2}{\partial x} & \frac{\partial N_3}{\partial y} & \frac{\partial N_3}{\partial x} & \frac{\partial N_4}{\partial y} & \frac{\partial N_4}{\partial x} & \frac{\partial N_5}{\partial y} & \frac{\partial N_5}{\partial x} & \frac{\partial N_6}{\partial y} & \frac{\partial N_6}{\partial x} \end{bmatrix}. \qquad (11)
$$

Also, as it is known that an LST element has a linear strain field, the element stiffness matrix can be given by,

$$
[k]^e = \int_v [B]^T [D][B] dv = \int_0^1 \int_{-0}^{1-L_1} [B]^T [D][B] t|J| dL_1 dL_2. \qquad (12)
$$

Nodal Displacement and Element Strain: The element stiffness matrices can subsequently be assembled into the global stiffness matrix $[K]$. The global stiffness matrix is a square matrix of dimension $[n \times DoF]$ where n is the total number of nodes in the system and DoF is the total degrees of freedom. With the global stiffness matrix, the nodal displacement matrix $\{U\}$ can be evaluated by,

$$
[K]\{U\} = \{F\}, \qquad (13)
$$

where $\{F\}$ is the global load vector of dimension $[nDoF \times 1]$.

Finally, the element strain $\{\varepsilon\}$, *for both 3 and 6-noded cases,* is calculated by,

$$
\{\varepsilon\} = [B]\{U\}. \qquad (14)
$$

Results:

A summary of the results for the MATLAB and ANSYS Mechanical APDL solutions is provided as well as the mesh convergence study and the Young's Modulus and loading condition sensitivity tests.

MATLAB Simulation: The nodal displacements for both the 3 and 6 noded cases are visualised in Figure 3 with the deformed shape super-imposed on the undeformed geometry. Table 1 contains all nodal displacement and element strain results from the MATLAB solution.

ANSYS Validation: The result from the ANSYS validation of the MATLAB solution is similarly visualised as a deformation plot overlayed on the undeformed geometry in Figure 4. Table 2 shows the nodal displacements and element strains for both element configurations of both the MATLAB and ANSYS solution, as well as the absolute error value between the results.

Mesh Convergence: The 6-noded triangular elements were chosen for the mesh convergence study with $E = 100$ GPa and $\theta = 90°$. Figure 5 shows the x, y and total displacement of nodes 4 and 5. Nodal displacement is a measurement of interest because one aim of this paper is to calculate nodal displacement, but also because nodes 4 and 5 are unsupported and therefore on average have a higher level of deformation than the other nodes. The grid independence study showed that nodal displacement reduced with decreasing element size, appearing to converge at an element size of approximately 0.001m for both nodes as the graph for x and y displacement plateaus in node 4 and 5. Therefore, the nodal displacement becomes independent of the mesh size at 0.001m global element size, or 5181 elements.

Additional Young's Moduli and Loading Conditions: Node 4 displacement and element 3 strain were chosen as query points for the effect of changing the Young's Modulus and loading angle. Table 3 shows the nodal displacement and element strain values for differing Young's Moduli and uniform tension loading angle, where one variable is changed and the other remains constant. A visualisation of these results is shown in Figure 6 where node 4 displacement and element 3 strain are plotted together.

Discussion:

An initial observation from Figure 3 shows that the 6-noded model has an overall higher level of deformation than the 3-noded model. This is consistent with the theory as under the same boundary conditions, 12 total nodes provide more opportunity for the structure to rotate about the nodes and subsequently flex along each plate edge. Furthermore, additional nodes may be able to better capture non-linear effects arising from the asymmetrical geometry. The general deformation shape is similar between both models as the maximum nodal displacement occurring in the x direction of node 5 for both. However, these values do differ, being only 7.02E-05m for the 3-noded elements and 1.27E-04m in the 6-noded model. For the element strain, the maximum strain in the 3-noded model is 1.75E-03 in the ε_x direction, but for the 6-noded model the maximum strain occurs in the γ_{xy} direction with a magnitude of 1.70E-02. It is therefore clear that the 6-noded model is experiencing a higher level of deformation overall.

As θ varies from $\theta = 0°$ to $\theta = 120°$, the displacement of node 4 in the y axis decreases, while the displacement of node 4 in the x axis increases. This is consistent with the theory because as θ increases from $0°$, the y component of the uniform tension decreases and the x component increases. Under the same change in θ, the element 3 strain in the ε_x and ε_y direction decrease, however there appears to be a linear increase in γ_{xy}. Again, as θ increases from $0°$, the component of uniform tension acting on the x axis of node 2 increases. Since only the x axis of node 2 is fixed, a constant uniform tension has to work against an increasing reaction force at node 2, decreasing the strain in element 3. This same effect causes element 3 to flex more at it's nodes, because node 1 is fully constrained, causing γ_{xy} to increase.

For a fixed loading angle of $\theta = 90°$, all components of node 4 displacement and element 3 strain appear to be inversely proportional to the Young's Modulus. This is because in Equation 7, the stress-strain relation matrix $[D]$ is directly proportional to E, and hence $[k]^e$ is also proportional. Therefore, Equation 13 and 14 show us that $[U]$ and $[\varepsilon]$ are inversely proportional to E.

Both the 3-noded and 6-noded models were replicated in ANSYS Mechanical APDL which showed very minimal absolute error against the MATLAB solution. The element strain average error for the 3-noded and 6-noded models respectively were 1.09E-08 and 5.97E-09. Also, the average nodal displacement absolute error was 2.01E-08m and 3.85E-10m for the 3 and 6 noded element configurations. This error is so small that it can be attributed to errors that naturally occur from rounding, floating point data, and numerical methods. Therefore, the MATLAB solution is validated because it was replicated identically in ANSYS Mechanical APDL.

Limitations: The first limitation is that the 3D plate is modelled as a thin 2D plate in plane stress. The z axis is therefore ignored. This could lead to vastly different behaviour under load, however the plate in 3D is likely to be uniform through the z axis so this assumption is appropriate in this case, and it is likely that we identified very similar behaviour patterns in this 2D plane stress model. Another limitation is that the numerical MATLAB model was verified by another numerical solver, both of which inherently use approximations. Ideally, real-world testing would be used to validate the MATLAB solution. Finally, we found that convergence was not reached until at least ~5181 elements in the 6-noded model. Thus, the three-element configuration would not be capable of producing a grid-independent result.

Conclusion: Both the 3-noded and 6-noded triangular element configurations were implemented in MATLAB and verified using ANSYS Mechanical APDL with negligible error. It was found that strain and displacement values from the 6-noded model were significantly more sensitive to the uniform tension and boundary conditions applied to the model. Therefore the 6-noded model may be more capable of capturing the deformation behaviour of the plate than the 3-noded model. These 3-element models were not grid independent however they still showed convincing results in finding the effect of changing Young's Modulus and loading direction on the strain and displacement.

References:

Akin, J. E. (2010). *Finite element analysis concepts: via SolidWorks.* World Scientific.

Ansys Inc. (2011). *ANSYS mechanical APDL element reference.* USA.

Ferreira, A. J. (2009). *MATLAB Codes for Finite Element Analysis.* Springer Netherlands.

Khennane, A. (2013). *Introduction to finite element analysis using MATLAB® and abaqus.* CRC Press.

Rao, S. S. (2017). The finite element method in engineering. Butterworth-heinemann.

Seshu, P. (2003). *Textbook of finite element analysis.* PHI Learning Pvt. Ltd.

Vanam, B. C. (2012). Static analysis of an isotropic rectangular plate using finite element analysis (FEA). *Journal of Mechanical Engineering Research* , 148-162.

W. E. Howard, J. C. (2001). Finite Element Analysis in a Mechanics Course Sequence. *Proceedings of the 2001 American Society for Engineering Education Annual Conference & Exposition.*

Figures and Tables Legend:

Figure 1: Diagram of the thin plate geometry, (x, y) coordinate system, uniform tension direction and magnitude, with corresponding loading angle θ.

Figure 2: Node and element placement for the **a)** 3-noded element configuration **b)** 6-noded element configuration.

Figure 3: Visualisation of the thin plate deformation under uniform tension solution from MATLAB, compared to the undeformed case, for both 3 and 6 noded element configurations. Displacement is exaggerated by a factor of 100 for clarity.

Figure 4: Visualisation of the thin plate deformation under uniform tension solution from ANSYS Mechanical APDL, compared to the undeformed case, for both 3 and 6 noded element configurations. Displacement is exaggerated by a factor of 100 for clarity.

Figure 5: Results of mesh convergence study for the x, y and total displacement of nodes 4 and 5 for varying global element edge lengths, of the 6-noded element configuration.

Figure 6: Plot of the x and y nodal displacements of node 4 and element 3 ε_x, ε_y and γ_{xy} strains under varying Young's Moduli and loading conditions; $E = \{50, 100, 150, 200, 250\}$ GPa and $\theta = \{0°, 30°, 60°, 90°, 120°\}$, for the 6-noded element configuration in MATLAB.

Table 1: Element strain $(\varepsilon_x, \varepsilon_y, \gamma_{xy})$ and nodal (x, y) displacement values for all elements and nodes in both the 3-noded and 6-noded element configurations.

Table 2: Element strain $(\varepsilon_x, \varepsilon_y, \gamma_{xy})$ and nodal (x, y) displacement values from the ANSYS Mechanical APDL simulation for both 3-noded and 6-noded element configurations, and their respective absolute error values when compared to the MATLAB results.

Table 3: Element strain $(\varepsilon_x, \varepsilon_y, \gamma_{xy})$ and nodal (x, y) displacement values for all elements and nodes in both the 3-noded and 6-noded element configurations, for varying Young's Moduli and loading conditions $E = \{50, 100, 150, 200, 250\}$ GPa and $\theta = \{0°, 30°, 60°, 90°, 120°\}$, with all other parameters fixed.

Figures and Tables:

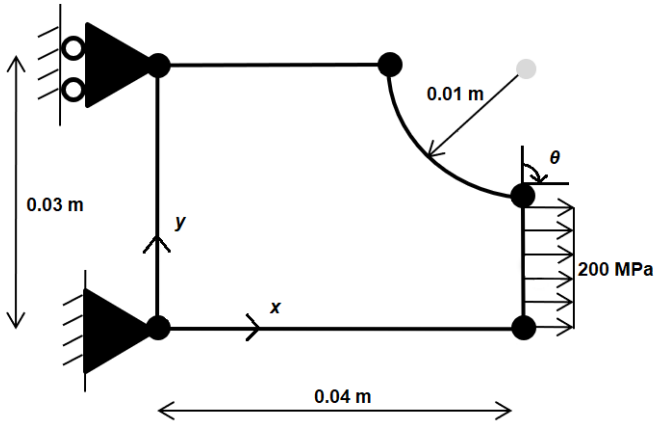

Figure 1

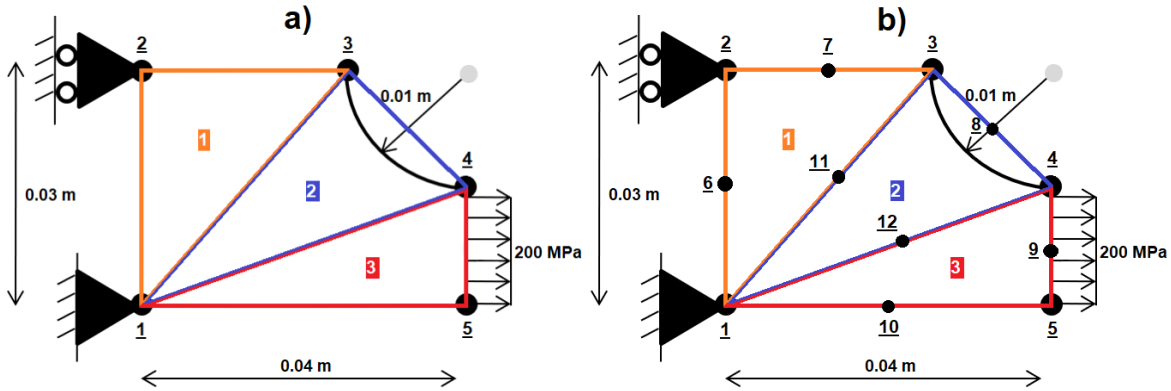

Figure 2

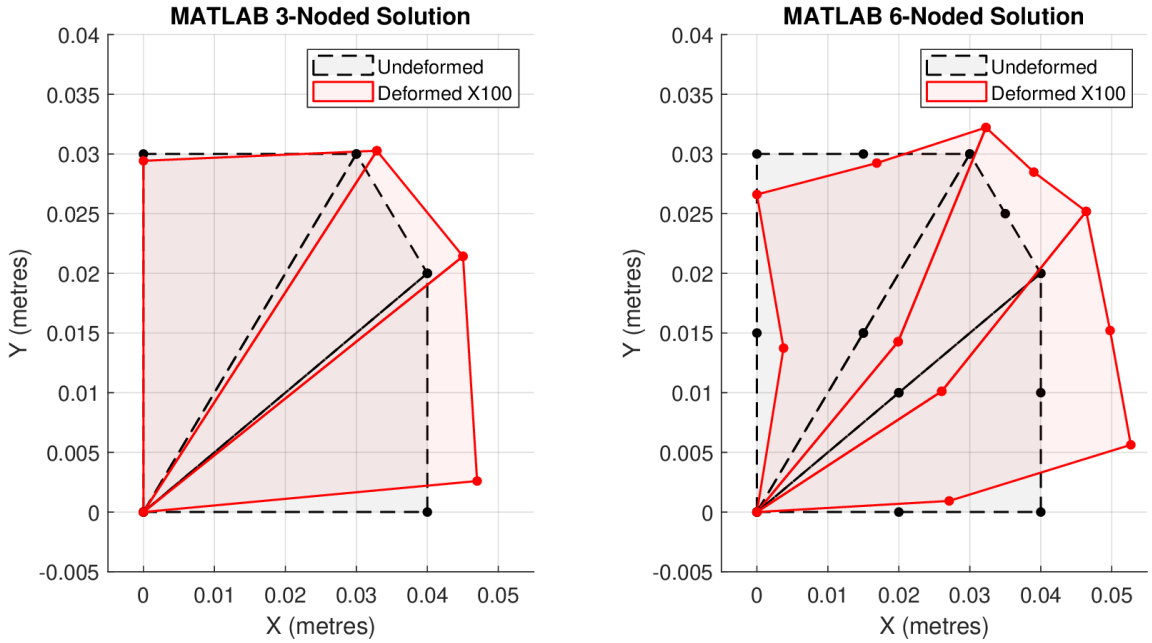

Figure 3

Strain			
Positions		Nodes Per Element	
Element	Direction	3	6
1	ε_x	9.65E-04	7.91E-04
1	ε_y	-1.91E-04	-1.09E-02
1	γ_{xy}	2.81E-04	-2.48E-03
2	ε_x	1.55E-03	4.30E-03
2	ε_y	-5.31E-04	2.30E-03
2	γ_{xy}	3.89E-05	7.59E-03
3	ε_x	1.75E-03	1.48E-02
3	ε_y	-5.87E-04	9.67E-03
3	γ_{xy}	-3.46E-04	1.70E-02
Displacement (meters)			
Positions		Nodes Per Element	
Node	Direction	3	6
1	u_x	0.00E+00	0.00E+00
1	u_y	0.00E+00	0.00E+00
2	u_x	0.00E+00	0.00E+00
2	u_y	-5.73E-06	-3.39E-05
3	u_x	2.89E-05	2.28E-05
3	u_y	2.72E-06	2.22E-05
4	u_x	5.02E-05	6.40E-05
4	u_y	1.43E-05	5.19E-05
5	u_x	7.02E-05	1.27E-04
5	u_y	2.60E-05	5.63E-05
6	u_x	-	3.76E-05
6	u_y	-	-1.27E-05
7	u_x	-	1.89E-05
7	u_y	-	-7.62E-06
8	u_x	-	4.02E-05
8	u_y	-	3.48E-05
9	u_x	-	9.76E-05
9	u_y	-	5.21E-05
10	u_x	-	7.10E-05
10	u_y	-	9.32E-06
11	u_x	-	4.90E-05
11	u_y	-	-7.24E-06
12	u_x	-	6.04E-05
12	u_y	-	1.20E-06

Table 1

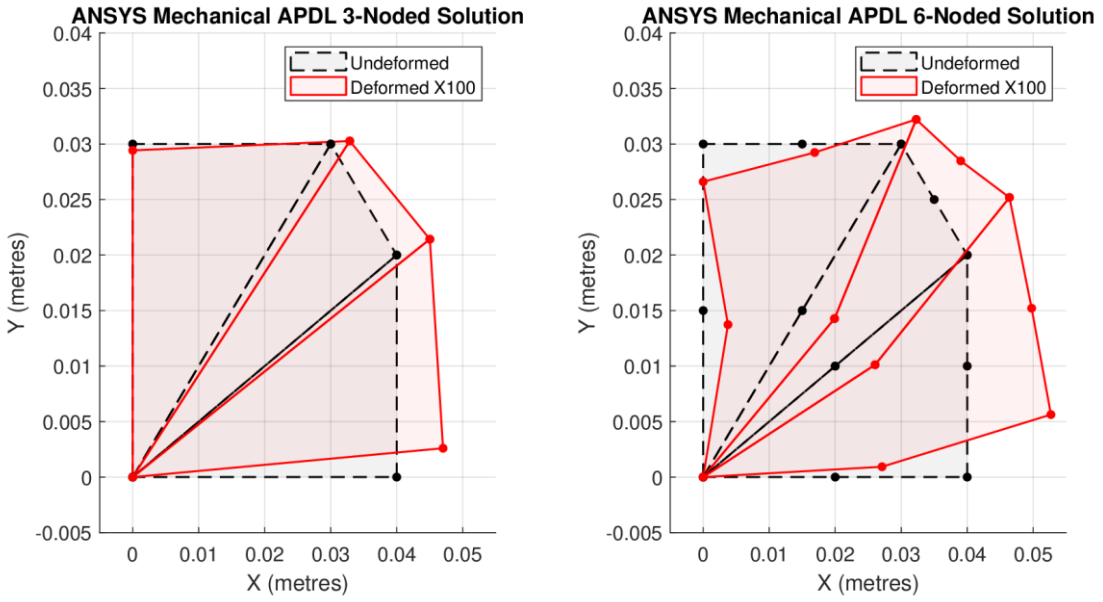

Figure 4

Strain							
Positions		MATLAB		ANSYS		3-Noded Absolute Error	6-Noded Absolute Error
Element	Direction	3-Node	6-Node	3-Node	6-Node		
1	ε_x	9.65E-04	7.91E-04	9.65E-04	7.91E-04	2.01E-09	9.31E-09
1	ε_y	-1.91E-04	-1.09E-02	-1.91E-04	-1.09E-02	2.44E-09	3.92E-09
1	γ_{xy}	2.81E-04	-2.48E-03	2.81E-04	-2.48E-03	4.75E-09	8.29E-09
2	ε_x	1.55E-03	4.30E-03	1.55E-03	4.30E-03	4.84E-08	1.82E-09
2	ε_y	-5.31E-04	2.30E-03	-5.31E-04	2.30E-03	3.08E-09	8.16E-09
2	γ_{xy}	3.89E-05	7.59E-03	3.89E-05	7.59E-03	2.06E-10	8.25E-09
3	ε_x	1.75E-03	1.48E-02	1.75E-03	1.48E-02	3.48E-08	8.35E-09
3	ε_y	-5.87E-04	9.67E-03	-5.87E-04	9.67E-03	8.20E-10	2.61E-09
3	γ_{xy}	-3.46E-04	1.70E-02	-3.46E-04	1.70E-02	1.31E-09	2.43E-09
Nodal Displacement (meters)							
Positions		MATLAB		ANSYS		3-Noded Absolute Error	6-Noded Absolute Error
Node	Direction	3-Node	6-Node	3-Node	6-Node		
1	u_x	0.00E+00	0.00E+00	0.00E+00	0.00E+00	0.00E+00	0.00E+00
1	u_y	0.00E+00	0.00E+00	0.00E+00	0.00E+00	0.00E+00	0.00E+00
2	u_x	0.00E+00	0.00E+00	0.00E+00	0.00E+00	0.00E+00	0.00E+00
2	u_y	-5.73E-06	-3.39E-05	-5.73E-06	-3.39E-05	3.37E-09	2.06E-10
3	u_x	2.89E-05	2.28E-05	2.89E-05	2.28E-05	4.00E-08	8.48E-11
3	u_y	2.72E-06	2.22E-05	2.72E-06	2.22E-05	2.67E-09	4.60E-10
4	u_x	5.02E-05	6.40E-05	5.02E-05	6.40E-05	4.84E-08	3.42E-10
4	u_y	1.43E-05	5.19E-05	1.43E-05	5.19E-05	4.88E-08	1.85E-10
5	u_x	7.02E-05	1.27E-04	7.02E-05	1.27E-04	4.26E-08	4.41E-09
5	u_y	2.60E-05	5.63E-05	2.60E-05	5.63E-05	1.48E-08	4.34E-10
6	u_x	-	3.76E-05	-	3.76E-05	-	2.03E-10
6	u_y	-	-1.27E-05	-	-1.27E-05	-	4.81E-10
7	u_x	-	1.89E-05	-	1.89E-05	-	1.95E-10
7	u_y	-	-7.62E-06	-	-7.62E-06	-	4.44E-11
8	u_x	-	4.02E-05	-	4.02E-05	-	3.99E-10
8	u_y	-	3.48E-05	-	3.48E-05	-	4.03E-10
9	u_x	-	9.76E-05	-	9.76E-05	-	3.80E-10
9	u_y	-	5.21E-05	-	5.21E-05	-	3.75E-11
10	u_x	-	7.10E-05	-	7.10E-05	-	4.04E-10
10	u_y	-	9.32E-06	-	9.32E-06	-	4.88E-11
11	u_x	-	4.90E-05	-	4.90E-05	-	1.79E-10
11	u_y	-	-7.24E-06	-	-7.24E-06	-	7.03E-12
12	u_x	-	6.04E-05	-	6.04E-05	-	3.17E-10
12	u_y	-	1.20E-06	-	1.20E-06	-	1.70E-11

Table 2

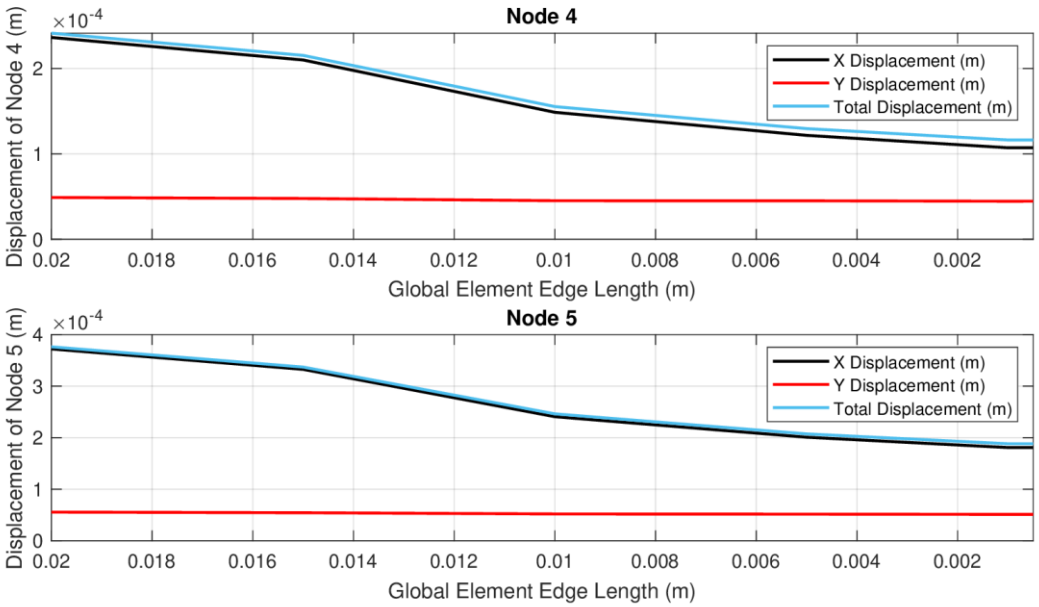

Figure 5

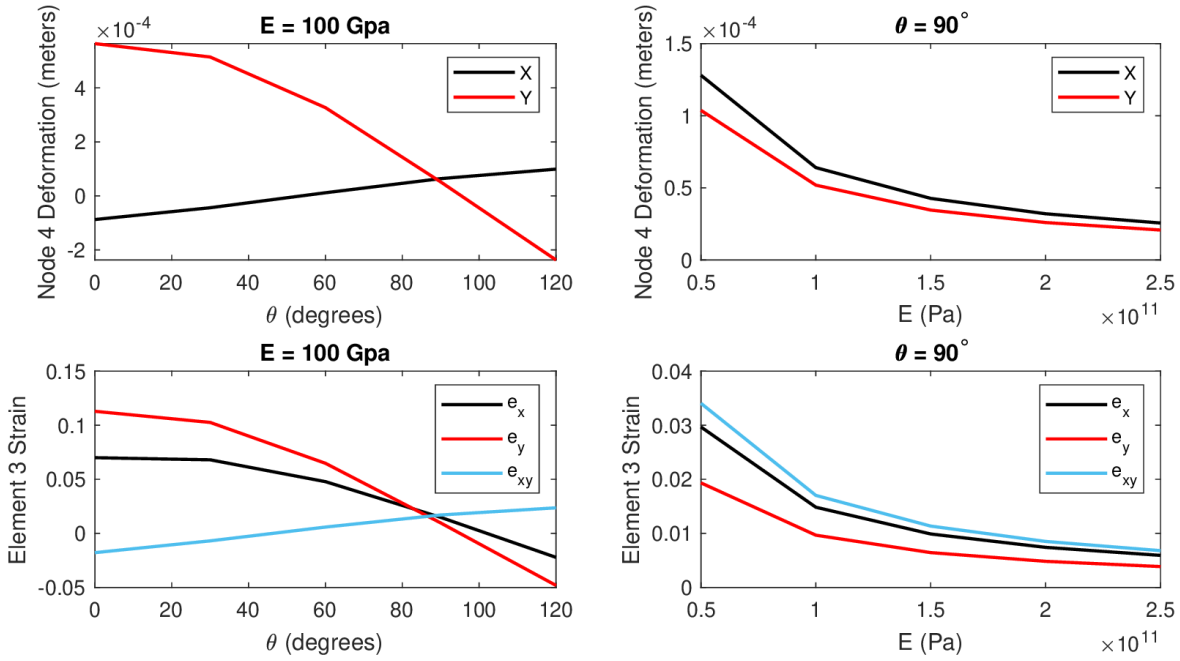

331 ***Figure 6***

Strain											
Positions		**Modulus of Elasticity (Gpa) (θ = 90°)**					**Loading Condition (Degrees) (E = 100Gpa)**				
Element	**Direction**	**E = 50**	**E = 100**	**E = 150**	**E = 200**	**E = 250**	**θ = 0°**	**θ = 30°**	**θ = 60°**	**θ = 90°**	**θ = 120°**
1	ε_x	1.58E-03	7.91E-04	5.27E-04	3.95E-04	3.16E-04	-4.12E-02	-3.53E-02	-1.99E-02	7.91E-04	2.13E-02
1	ε_y	-2.19E-02	-1.09E-02	-7.30E-03	-5.47E-03	-4.38E-03	-3.71E-02	-3.76E-02	-2.80E-02	-1.09E-02	9.07E-03
1	γ_{xy}	-4.96E-03	-2.48E-03	-1.65E-03	-1.24E-03	-9.91E-04	9.40E-02	8.02E-02	4.49E-02	-2.48E-03	-4.92E-02
2	ε_x	8.61E-03	4.30E-03	2.87E-03	2.15E-03	1.72E-03	7.22E-04	2.78E-03	4.09E-03	4.30E-03	3.37E-03
2	ε_y	4.60E-03	2.30E-03	1.53E-03	1.15E-03	9.19E-04	4.56E-02	4.06E-02	2.48E-02	2.30E-03	-2.08E-02
2	γ_{xy}	1.52E-02	7.59E-03	5.06E-03	3.80E-03	3.04E-03	2.05E-02	2.15E-02	1.68E-02	7.59E-03	-3.65E-03
3	ε_x	2.97E-02	1.48E-02	9.89E-03	7.42E-03	5.94E-03	7.00E-02	6.80E-02	4.78E-02	1.48E-02	-2.21E-02
3	ε_y	1.93E-02	9.67E-03	6.45E-03	4.84E-03	3.87E-03	1.13E-01	1.03E-01	6.48E-02	9.67E-03	-4.81E-02
3	γ_{xy}	3.41E-02	1.70E-02	1.14E-02	8.51E-03	6.81E-03	-1.78E-02	-6.90E-03	5.85E-03	1.70E-02	2.36E-02
Nodal Displacement (meters)											
Positions		**Modulus of Elasticity (Gpa) (θ = 90°)**					**Loading Condition (Degrees) (E = 100Gpa)**				
Node	**Direction**	**E = 50**	**E = 100**	**E = 150**	**E = 200**	**E = 250**	**θ = 0°**	**θ = 30°**	**θ = 60°**	**θ = 90°**	**θ = 120°**
1	u_x	0.00E+00	0.00E+00	0.00E+00	0.00E+00	0.00E+00	0.00E+00	0.00E+00	0.00E+00	0.00E+00	0.00E+00
1	u_y	0.00E+00	0.00E+00	0.00E+00	0.00E+00	0.00E+00	0.00E+00	0.00E+00	0.00E+00	0.00E+00	0.00E+00
2	u_x	0.00E+00	0.00E+00	0.00E+00	0.00E+00	0.00E+00	0.00E+00	0.00E+00	0.00E+00	0.00E+00	0.00E+00
2	u_y	-6.79E-05	-3.39E-05	-2.26E-05	-1.70E-05	-1.36E-05	1.15E-04	8.25E-05	2.80E-05	-3.39E-05	-8.68E-05
3	u_x	4.55E-05	2.28E-05	1.52E-05	1.14E-05	9.10E-06	-2.01E-04	-1.63E-04	-8.10E-05	2.28E-05	1.20E-04
3	u_y	4.43E-05	2.22E-05	1.48E-05	1.11E-05	8.87E-06	3.85E-04	3.44E-04	2.12E-04	2.22E-05	-1.73-E-04
4	u_x	1.28E-04	6.40E-05	4.27E-05	3.20E-05	2.56E-05	-8.75E-05	-4.37E-05	1.17E-05	6.40E-05	9.92E-05
4	u_y	1.04E-04	5.19E-05	3.46E-05	2.59E-05	2.07E-05	5.64E-04	5.14E-04	3.27E-04	5.19E-05	-2.37E-04
5	u_x	2.54E-04	1.27E-04	8.46E-05	6.34E-05	5.07E-05	2.09E-04	2.45E-04	2.15E-04	1.27E-04	5.12E-06
5	u_y	1.13E-04	5.63E-05	3.76E-05	2.82E-05	2.25E-05	5.80E-04	5.31E-04	3.39E-04	5.63E-05	-2.41E-04
6	u_x	7.51E-05	3.76E-05	2.50E-05	1.88E-05	1.50E-05	-1.56E-05	5.25E-06	2.47E-05	3.76E-05	4.03E-05
6	u_y	-2.53E-05	-1.27E-05	-8.44E-06	-6.33E-06	-5.06E-06	5.78E-05	4.37E-05	1.79E-05	-1.27E-05	-3.99E-05
7	u_x	3.78E-05	1.89E-05	1.26E-05	9.44E-06	7.55E-06	-1.26E-04	-9.97E-05	-4.66E-05	1.89E-05	7.94E-05
7	u_y	-1.52E-05	-7.62E-06	-5.08E-06	-3.81E-06	-3.05E-06	1.83E-04	1.55E-04	8.49E-05	-7.62E-06	-9.81E-05
8	u_x	8.05E-05	4.02E-05	2.68E-05	2.01E-05	1.61E-05	-1.51E-04	-1.11E-04	-4.06E-05	4.02E-05	1.10E-04
8	u_y	6.96E-05	3.48E-05	2.32E-05	1.74E-05	1.39E-05	4.67E-04	4.22E-04	2.64E-04	3.48E-05	-2.03E-04
9	u_x	1.95E-04	9.76E-05	6.51E-05	4.88E-05	3.91E-05	4.86E-05	9.09E-05	1.09E-04	9.76E-05	6.02E-05
9	u_y	1.04E-04	5.21E-05	3.47E-05	2.60E-05	2.08E-05	5.71E-04	5.21E-04	3.31E-04	5.21E-05	-2.40E-04
10	u_x	1.42E-04	7.10E-05	4.73E-05	3.55E-05	2.84E-05	1.43E-04	1.60E-04	1.33E-04	7.10E-05	-1.02E-05
10	u_y	1.86E-05	9.32E-06	6.22E-06	4.66E-06	3.73E-06	2.47E-04	2.18E-04	1.32E-04	9.32E-06	-1.15E-04
11	u_x	9.80E-05	4.90E-05	3.27E-05	2.45E-05	1.96E-05	-2.49E-05	2.97E-06	3.00E-05	4.90E-05	5.49E-05
11	u_y	-1.45E-05	-7.24E-06	-4.82E-06	-3.62E-06	-2.89E-06	1.67E-04	1.41E-04	7.74E-05	-7.24E-06	-8.99E-05
12	u_x	1.21E-04	6.04E-05	4.03E-05	3.02E-05	2.42E-05	2.42E-05	5.12E-05	6.44E-05	6.04E-05	4.02E-05
12	u_y	2.40E-06	1.20E-06	8.00E-07	6.00E-07	4.80E-07	2.34E-04	2.03E-04	1.18E-04	1.20E-06	-1.16E-04

332 ***Table 3***